Toward the Advanced Manufacturing of Land-Based Wind Turbine Blades

Preprint

Pietro Bortolotti,[1] Derek Berry,[1] William Scott Carron,[1] Sherif Khalifa,[1] Todd Anderson,[2] Pascal Meyer,[2] and Molly Chann[3]

1 National Renewable Energy Laboratory
2 GE Global Research
3 GE Renewable Energy

Presented at the 2023 American Institute of Aeronautics and Astronautics SciTech Forum
National Harbor, Maryland
January 23–27, 2023

NREL is a national laboratory of the U.S. Department of Energy
Office of Energy Efficiency & Renewable Energy
Operated by the Alliance for Sustainable Energy, LLC

This report is available at no cost from the National Renewable Energy Laboratory (NREL) at www.nrel.gov/publications.

Contract No. DE-AC36-08GO28308

Conference Paper
NREL/CP-5000-84397
December 2022

Toward the Advanced Manufacturing of Land-Based Wind Turbine Blades

Preprint

Pietro Bortolotti,[1] Derek Berry,[1] William Scott Carron,[1] Sherif Khalifa,[1] Todd Anderson,[2] Pascal Meyer,[2] and Molly Chann[3]

1 National Renewable Energy Laboratory
2 GE Global Research
3 GE Renewable Energy

Suggested Citation
Bortolotti, Pietro, Derek Berry, William Scott Carron, Sherif Khalifa, Todd Anderson, Pascal Meyer, and Molly Chann. 2022. *Toward the Advanced Manufacturing of Land-Based Wind Turbine Blades: Preprint*. Golden, CO: National Renewable Energy Laboratory. NREL/CP-5000-84397. https://www.nrel.gov/docs/fy23osti/84397.pdf.

NREL is a national laboratory of the U.S. Department of Energy
Office of Energy Efficiency & Renewable Energy
Operated by the Alliance for Sustainable Energy, LLC

This report is available at no cost from the National Renewable Energy Laboratory (NREL) at www.nrel.gov/publications.

Contract No. DE-AC36-08GO28308

Conference Paper
NREL/CP-5000-84397
December 2022

National Renewable Energy Laboratory
15013 Denver West Parkway
Golden, CO 80401
303-275-3000 • www.nrel.gov

NOTICE

This work was authored in part by the National Renewable Energy Laboratory, operated by Alliance for Sustainable Energy, LLC, for the U.S. Department of Energy (DOE) under Contract No. DE-AC36-08GO28308. Funding provided by the U.S. Department of Energy Office of Energy Efficiency and Renewable Energy Advanced Materials and Manufacturing Technologies Office. The views expressed herein do not necessarily represent the views of the DOE or the U.S. Government. The U.S. Government retains and the publisher, by accepting the article for publication, acknowledges that the U.S. Government retains a nonexclusive, paid-up, irrevocable, worldwide license to publish or reproduce the published form of this work, or allow others to do so, for U.S. Government purposes.

Cover Photos by Dennis Schroeder: (clockwise, left to right) NREL 51934, NREL 45897, NREL 42160, NREL 45891, NREL 48097, NREL 46526.

Toward the Advanced Manufacturing of Land-Based Wind Turbine Blades

Pietro Bortolotti*, Derek Berry†, William Scott Carron‡, and Sherif Khalifa§
National Renewable Energy Laboratory, Golden, CO, 80401, USA

Todd Anderson¶ and Pascal Meyer‖
GE Global Research, Niskayuna, NY, 12309, USA

Molly Chann**
GE Renewable Energy, New Orleans, LA, 70122, USA

The National Renewable Energy Laboratory and General Electric (GE) are partners within the Additive and Modular-Enabled Rotor Blades and Integrated Composites Assembly (AMERICA) project. AMERICA aims to develop advanced manufacturing solutions to reduce labor and cycle time while increasing recyclability of wind turbine blades. The project is funded by the U.S. Department of Energy's Advanced Manufacturing Office. This paper describes the techno-economic and life cycle analysis of the novel manufacturing process applied to the 15-meter long tip of the blade of a representative 3.4 MW land-based wind turbine. We establish a comparison to a standard manufacturing process, highlighting challenges and opportunities. Several uncertainties affect the analysis, but we highlight an opportunity space. With the current set of assumptions, the tip adopting advanced manufacturing is predicted to lower labor by 21%, cycle time by 39%, and total blade tip costs by 15% while simultaneously increasing production quality and adopting recyclable thermoplastic resin. A life cycle analysis returns comparable metrics for climate change impact and embodied energy between the two processes.

I. Background, Motivation, and Goals

The path toward lower levelized cost of wind energy goes through larger rotors and taller towers [1, 2]. Longer blades and higher hub heights increase the energy capture per turbine and offer higher availability of wind power in the electricity mix. The wind turbine market clearly shows the increase in turbine size, both offshore and land-based. Wind turbine operators tend to order larger machines to limit the number of installations, which helps lower balance-of-station costs and operation and maintenance costs. In this scenario, wind turbine blade manufacturers fight the cubic growth of mass and cost with respect to blade length. In the past decade, manufacturers have been successful keeping the growth exponent closer to 2 than 3 thanks to materials advancements, such as using pultruded carbon fiber spar caps, and active and passive load alleviation technologies. In parallel, the end-of-life treatments of wind turbine blades is a primary concern, and the motivation to design and manufacture recyclable blades is growing [3]. In this scenario, industry and researchers are busy investigating the technologies that will support the next generation of wind turbine rotors [4].

A promising pathway consists of increasing the level of automation in the manufacturing of wind turbine blades. Today, blades are manufactured via vacuum-assisted resin transfer molding (VARTM) and production is characterized by high values of labor hours and cycle time, low factory throughput, inconsistent production quality, and low to no recycling [5, 6]. In addition, the resin uptake within the sandwich composite cores located within the skins and shear webs of the blade results in a mass and cost penalty [7]. Process automation and reduced resin uptake penalties using additive manufacturing processes could enable higher-performance structures with lower labor, material, and manufacturing costs [8–10]. Additive manufacturing, or 3D printing, differs from conventional blade manufacturing in that the structures are manufactured directly from computer-aided design (CAD) models in a layer-by-layer fashion [11].

*Research Engineer, National Wind Technology Center
†Senior Research Engineer, National Wind Technology Center
‡Senior Research Engineer, National Wind Technology Center
§Research Engineer, National Wind Technology Center
¶Principal Mechanical Engineer
‖Senior Engineer - Structures
**Senior Manager - Advanced Manufacturing Technology

Material extrusion is the process of extruding polymers and fiber-reinforced polymers through a nozzle to deposit a bead and fuse it to the previous layer. Thermoplastics are the predominant choice of feedstock, although thermosetting polymers are being investigated to increase part strength through additional cross-linking effects [12]. Thermoplastic feedstocks such as acrylonitrile butadiene styrene (ABS), polylactic acid (PLA), nylon, and glycol-modified polyethylene terephthalate (PETg) are widely used due to the extruder requirements, their low glass transition temperatures, and recyclability [11, 13]. Discontinuous fibers, such as carbon fiber, in the range of 150 micrometers in length to prevent breakage within the extruder are commonly added to the feedstock to increase the strength and stiffness, as well as retain heat and provide dimensional stability [10, 14, 15]. Small-scale material extrusion technologies use filament feedstock, whereas large-scale technologies utilize pelletized feedstock to reduce cost [10]. Industry adoption of material extrusion has been successful within tooling and rapid prototyping applications [15]. Expanding polymer-based material extrusion into functional structures, such as wind turbine blades, is a challenge. Open research questions include how to achieve required mechanical properties, interlayer shear strength, fiber sizing, and compatible structural adhesives. There is also a lack of standards, certification, anisotropic behavior, material voids, serial production cost, overall part quality, and additive manufacturing workforce [11, 13, 15–21]. Despite these challenges, the potential of additive manufacturing to provide novel structural solutions is indicated by continued patent filings [22–25], government-based research [26, 27], and advancement of additive manufacturing standardization [18].

This paper investigates potential and challenges of a novel advanced and additive manufacturing process for wind turbine blades, with a focus on the tip region, whose lightweight and strict tolerance requirements are key to minimize the levelized cost of energy generated by wind turbines. The outer blade span generates the highest contribution to annual energy production. While the inner portion of the blade can be characterized by cost-efficient processes that focus on the structure, blade tips benefit from processes characterized by a high level of precision to manufacture accurate aerodynamic shapes. This critical difference in the manufacturing objective suggests that blade tips could be manufactured in a different way compared to the rest of the structure. Blade tips could also be manufactured with a high degree of automation in a market with high labor rates, whereas the inner blade section could be manufactured in lower-cost markets. The two blade portions could then be transported separately, thus alleviating logistics constraints and supporting larger rotor diameters, and assembled on-site thanks to a spanwise joint system. Finally, blade tips have less demanding structural requirements than inboard, offering a feasible path to thermoplastic composites, which, different from thermoset composites, can be melted and reutilized at the end of life of the blade .

This study focuses on an 80-m-long segmented wind turbine blade representative of modern land-based configurations. The study leverages the National Renewable Energy Laboratory's open-source systems engineering framework, the Wind-Plant Integrated System Design and Engineering Model (WISDEM®), and its detailed blade manufacturing and cost model [5]. This model was first adapted to model a segmented blade and was later extended to model advanced manufacturing processes. In addition, an attributional process-based life cycle assessment investigation following the International Organization for Standardization (ISO 14040/44) framework is carried out. The goal of this activity is to compare the environmental impacts of baseline and advanced manufacturing processes [28]. We select a cradle-to-gate system boundary that encompasses life cycle stages from primary material acquisition to the exit gate of a blade manufacturing facility. This analysis currently excludes the potential recyclability or other performance benefits (e.g., increase in energy yield) for both tip designs. Also, labor, research and development, and other miscellaneous activities are left outside of the system boundary due to considerable uncertainty in labor footprint data.

The paper is organized as follows. Section II introduces the key characteristics of the baseline wind turbine manufactured via conventional processes. Next, Section III presents the advanced manufacturing model, Section IV discusses the comparison between the two processes, and Section V compares the results from the life cycle analysis. Finally, Section VI summarizes the key takeaways of the study.

II. Design and Manufacturing of a Conventional Segmented 80-m Blade

The 80-m-long segmented wind turbine blade design was developed starting from the International Energy Agency (IEA) Wind Task 37 land-based reference wind turbine [29]. The key characteristics of the turbine adopted in this study are listed in Table 1. The key differences between the IEA land-based reference turbine and the baseline design adopted in this work are the higher hub height, increased from 110 to 120 m, and the significantly larger rotor, whose blades are extended from 63 to 80 m. Rated power is kept constant at 3.4 MW, and specific power is consequently reduced from 250 to 161 W m^{-2}, in line with the predictions presented by [1]. The rotor tip speed ratio is increased from 8 to 10, and the maximum blade tip speed from 80 m s^{-1} to 85 m s^{-1}. Also, the spar caps are changed from standard infused glass fiber to 300-mm-wide pultruded carbon fiber. Finally, rotor precone, nacelle uptilt, and rotor overhang are increased to 4

Table 1 Summary of the key turbine characteristics assumed in the study

Metric	Value	Metric	Value
Wind Class	3A	Nameplate power (MW)	3.4
Rotor diameter (m)	164	Specific power (W m^{-2})	161
Hub height (m)	120	Gearbox ratio	120
Generator	DFIG	Rotor overhang (m)	6
Rotor cone angle (deg)	4	Nacelle uptilt angle (deg)	6
Cut in (m s^{-1})	3	Cut out (m s^{-1})	25

degrees, 6 degrees, and 6 m, respectively, all to support lighter and more flexible blades. The drivetrain is made of a gearbox with a ratio of 1:120 coupled to a doubly-fed induction generator (DFIG). The next subsections discuss other key aspects of the blade design.

A. Root

The blade root represents a major contribution to blade mass and cost. In this work, blade root diameter was assumed equal to 4 m. This value is possibly slightly larger than necessary for an 80-m blade, but it was chosen to simulate the modularization of the inner portion of the blade. This approach is an available pathway for turbine blade manufacturers to take advantage of economies of scale and design a single blade inner portion that can support blade tips of various lengths. The composite layup at blade root is composed of a combination of triaxial and unidirectional glass fabrics to house the welded root bushings. The maximum laminate thickness at the root of the blade is 75.8 mm, and blade and hub are connected via 84 root bolts. Note that the design of blade root bushings could be a topic of further investigation to optimize the design, since the potential for blade mass reduction is large.

B. Spanwise Joint

Increasing blade length from 63 to 80 m not only requires a redesign process, but longer blades also face tighter logistics constraints. These can be overcome with various technological solutions [30–32]:

1) Spanwise segmentation
2) Controlled flexing during rail transport
3) On-site manufacturing
4) Airship transport.

This work assumes the first solution, which is the only commercially ready among the four. Controlled flexing and on-site manufacturing are considered promising technologies, but are characterized by lower technology readiness levels. Airship transport of large wind turbine components could be a game changer but has not been proven at the scale of wind turbine blades. A wide spectrum of wind turbine blade joints has been proposed in the literature, and their technical viability have been demonstrated in the field [33]. On one end of the spectrum, lightweight composite joints offer an opportunity for modular manufacturing but usually require a factory-assembling step and are therefore not suitable to address logistics constraints. Mechanical joints, in either bolted or pin configuration, are instead usually heavier, but successfully support field assembly. In this work, a bolted joint is assumed and sized according to [34]. The joint is located 65 m away from the blade root—i.e., at 81.25% of blade span. The bolted joint is composed of 22 M24 bolts—i.e., 11 per side. The bolts are embedded into a triaxial glass fiber laminate that runs over a span of 10 m and whose width varies linearly between 300 mm at the start and end and 800 mm at the joint location. The 22 bolts and the extra laminate to house them are estimated to weigh 121 kg and 358 kg, respectively, for a total joint mass of 479 kg.

C. Lightning Protection

Mechanical joints are often made of metal, which, combined with the pultruded carbon fiber spar caps, represent a challenge for lightning protection. Also, lightning protection systems are increasingly expensive. In this work, the lightning protection system is estimated to weigh 68 kg and cost $2,700 (USD). In addition, the spar cap assemblies of pultruded planks are modeled to stop at 90% of blade span and transition to standard VARTM unidirectional glass fiber for the last 8 m of blade span.

D. Changes to Cost Model

During the project, the blade cost model described in [5] was improved to model two manufacturing processes for the blade inner portion and the blade tip. In addition, the model was extended to account for spar caps made of pultruded planks. This consisted of first removing the separate infusion processes for the spar caps and the corresponding tooling and equipment costs. Next, three new steps were included: loading the coil into position, cutting and chamfering pultrusion planks, and stacking the planks. A team of four workers per spar cap is assumed. The first step is assumed to last thirty minutes. The second step is assumed to run at a rate of six planks per hour. The last step of stacking the planks is assumed to run at 15 planks per hour, plus loading, moving, and placing steps that last 30, 15, and 30 minutes, respectively. The pultruded planks also required extra equipment, with corresponding costs. The model assumes a cutting and chamfering unit with a cost of \$200,000, a stacking table that costs \$100 m^{-1} per spar cap length, and a fixture unit that costs \$200 m^{-1} per spar cap length. Finally, the unburdened labor rate was increased from \$20 h^{-1} to \$35 h^{-1} assuming a typical wind blade production facility position in the United States.

E. Aerostructural Design Optimization

Once the changes described in the previous subsections were implemented, an aerostructural design process was run in WISDEM. Design variables controlled chord, twist, and spar cap thickness along the blade span, whereas constraints ensured the blade did not experience stall, did not exceed strains above 3,500 microstrains, did not violate the minimum blade-tower clearance, and limited the nondimensional blade root flapwise moment coefficient to 0.165 [35]. The figure of merit was levelized cost of energy, and the financial model in WISDEM was tuned based on the most recent numbers from [36]. The design optimization returns a total blade mass of 20,300 kg and a total blade cost of \$294,900. The turbine annual energy production is 16.3 GWh. All these values are expected to be in line with industrial rotors for Class 3 wind conditions. The input to the financial model of WISDEM and the output levelized cost of energy are reported in Table 2. The plots in Fig. 1 show the comparison in terms of chord, twist, axial induction profile, and mass distribution between the 63-m-long blade design from the IEA Wind Task 37 land-based reference turbine and the new segmented 80-m-long design. Note the low solidity of the blade generated by the tip speed ratio of 10 and the low induction profile caused by the constraint on blade root flapwise moment. The low mass distribution is supported by the use of carbon fiber spar caps and the increased values of blade tower clearance. The uptick in mass at 65-m span corresponds to the spanwise location of the joint.

Table 2 Levelized cost of energy and key financial metrics

Metric	Value	Metric	Value
Turbine capital (\$ kW^{-1})	1,415	Plant capacity (MW)	600
Balance of stations (\$ kW^{-1})	217	Turbine number	178
Turbine annual energy production (GWh)	16.3	Operating expenses (\$ kW^{-1})	43
Fixed charge rate (%)	6.5	Wake loss factor (%)	15
		Levelized cost of energy (\$ MWh^{-1})	36.5

F. Costs, Labor, and Cycle Time of Conventional Manufacturing

The optimum blade design identified by WISDEM returned variable and fixed costs as listed in Tables 3 and 4. Labor consisted of 1,153 hours (h) for the inner portion and 156 h for the blade tip. The model split cycle time between gating—the cycle time happening at the main mold, representing the bottleneck of factory throughput—and non-gating, which consists of all those operations that can happen in parallel and do not usually limit production. The blade inner portion is set to run on a 24-h gating cycle time and the tip on a 12-h gating cycle time. A detailed techno-economic analysis estimates that the inner blade portion and the tip have total costs of \$274,200 and \$20,700, respectively, for a total blade cost of \$294,900. Figure 2 shows the cost share distribution for the 15-m-long blade tip.

Table 3 Labor, cycle time, and variable costs of the blade manufactured via conventional methods, split between inner portion and tip

Metric	Inner	Tip	Total
Total labor (h)	1,153	156	1,309
Skin mold cycle time (h)	24	12	36
Non-gating cycle time (h)	140	47	187
Total labor cost ($K)	68.1	9.2	77.3
Root bolts and lightning protection system ($K)	5.8	1.4	7.3
Consumables ($K)	7.2	1.3	8.5
Utility costs ($K)	0.9	0.0	0.9
Laminates and foam ($K)	154.5	7.4	161.9
Total variable costs ($K)	223.5	16.6	240.1

Table 4 Fixed and total costs of the blade manufactured via conventional methods, split between inner portion and tip.

Metric	Inner	Tip	Total
Equipment ($K)	4.4	0.3	4.7
Tooling ($K)	10.7	0.2	10.9
Building ($K)	0.6	0.02	0.6
Maintenance ($K)	4.2	0.4	4.6
Overhead ($K)	20.4	2.8	23.2
Capital ($K)	10.4	0.6	11.0
Total blade fixed cost ($K)	50.7	4.1	54.8
Total costs ($K)	274.2	20.7	294.9

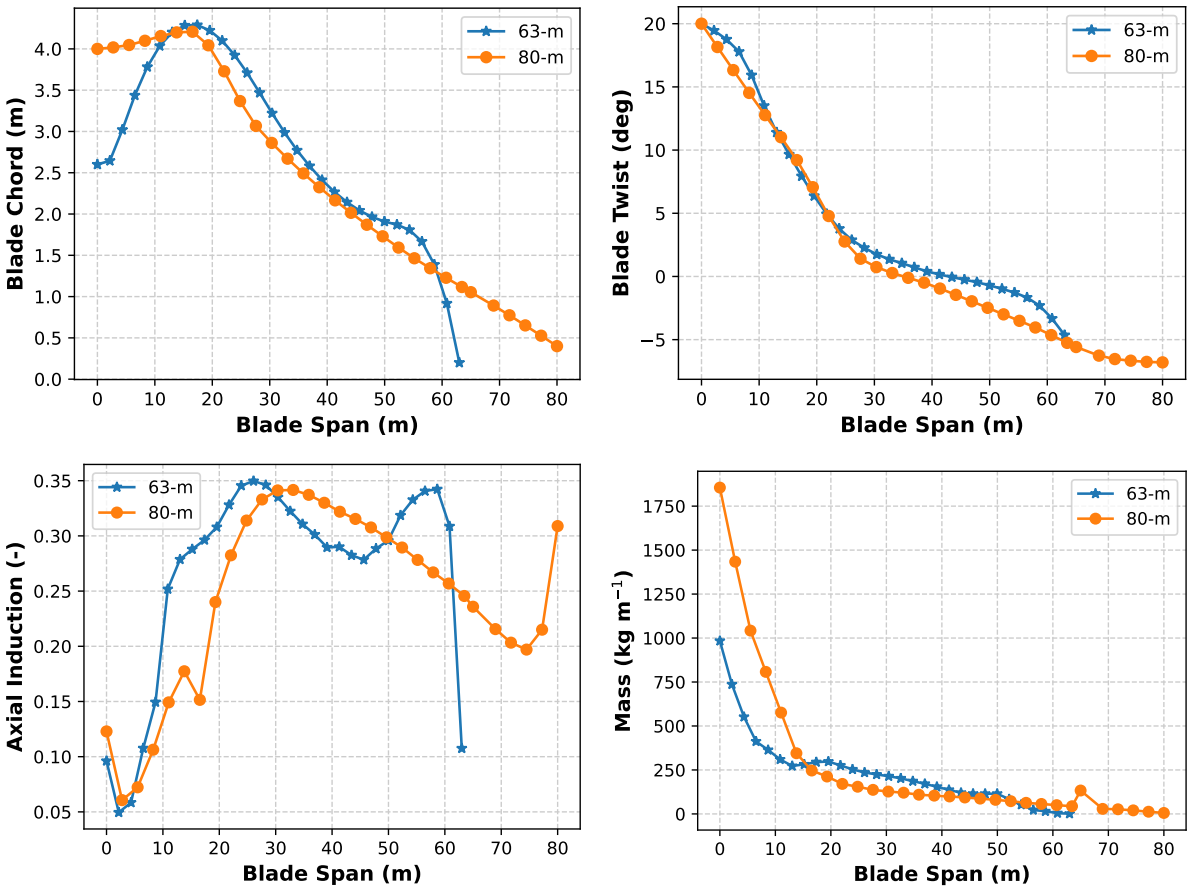

Fig. 1 Comparison in terms of chord, twist, axial induction profile, and mass distribution between the 63-m-long blade design from the IEA Wind Task 37 land-based reference turbine and the new segmented 80-m-long design.

III. Advanced Manufacturing of the 15-m Blade Tip

The advanced manufacturing process assumed in this study changes the way the blade tip is designed and manufactured. In a conventional manufacturing process, a blade is made of two shells made of composite sandwich structures comprising an inner and outer fabric infused with thermoset resin and a lightweight foam or balsa wood core. In the advanced manufacturing process, skins are first pre-infused with an in-situ polymerizing thermoplastic resin on a flat table and then thermoformed into the mold using a vacuum process. Once in position, 3D printers perform the additive manufacturing of panel reinforcements to increase buckling resistance. The reinforcement has a honeycomb structure and is made of thermoplastic material with chopped glass fibers. The assembly is assumed to rely on conventional bond lines, although in the future, heat-activated film adhesive and thermal welding will be considered. Note that the focus of this paper is on the techno-economic analysis, but detailed 3D finite element analyses were conducted to ensure that the AM tip meets the same structural requirements of the baseline tip.

This advanced manufacturing (AM) process impacts several aspects in the areas of materials selection, structural design, and manufacturing. In this study, only blade tips adopt AM, whereas future research will study the impact of AM on the inner portion of the blade. The following subsections describe each subprocess.

A. Prefabricated Tip Blanks

Prefabricating tip blanks consists of infusing a stack of dry unidirectional, biaxial, and triaxial layers of glass fiber with a thermoplastic resin on a flat table. The planks for the pultruded spar caps are also laid on the dry fabric and infused so that resin bonds everything together. This infusion is similar to the conventional infusion happening in the mold, except that flat blanks are easier to handle on a flat table than in a curved mold. Flat tables are assumed to be

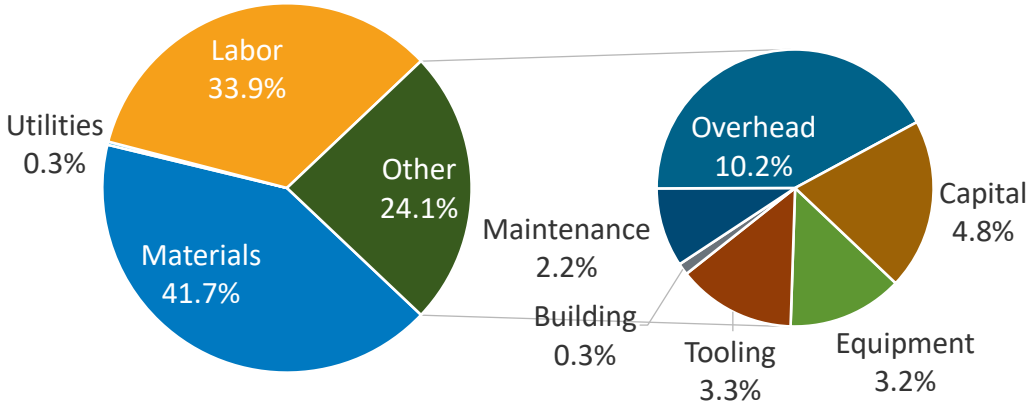

Fig. 2 Cost shares of the 15-m blade tip manufactured via the conventional process. Total cost per tip is $20,700.

non-heated, cost \$2,000 m^{-2}, and be usable for 6,000 infusions. Fabric layout and lifting fixtures are also modeled with an estimated cost of \$9,500. A unit cost of \$6.83 kg^{-1} is assumed for the in-situ polymerizing thermoplastic resin. The model assumes that the three steps of cutting, molding, and trimming are conducted by a team of two people. The total labor is estimated to be 16.5 h per skin and 33 h per tip, for a total labor cost of \$1,200. Note that blade manufacturers might decide to keep the step of prefabricating tip blanks internal, but since they would not need to share proprietary airfoil shapes and 3D geometries, they could also decide to outsource the step and simply purchase prefabricated flat tip blanks from suppliers.

B. Vacuum Thermoforming of Skin Panels

The vacuum thermoforming of skin panels consists of applying a vacuum bag on top of the flat tip blanks and forming the thermoplastic layers into the blade tip shell. Molds are heated during the thermoforming process, and a unit tooling cost of \$8,500 m^{-2} is assumed. Molds are assumed to be used for 3,000 tips, whereas consumables costs are estimated to be \$250 per tip. The process is completed by four workers with a total labor time of 17 h and a cycle time per skin of 2 h. Labor costs equal \$583 per blade tip.

C. Additive Manufacturing of Outer Shell Reinforcement

The additive manufacturing of the buckling reinforcement of the blade tip outer shell is a sophisticated process that offers an opportunity to reduce labor and cycle time and increase production quality. Given a volume of grid material for a required equivalent panel stiffness, a material density of 1,700 kg m^{-3}, and a grid density of 300 kg m^{-3}, 40 kg of grid reinforcement is estimated. The maximum deposition rate for the material extruder is assumed equal to 5 kg h^{-1}, bead height equal to 2.5 mm, and 16 extruders running in parallel, leading to an effective deposition rate of 80 kg h^{-1} and a total deposition time of 17 minutes per half shell. The total 3D print time is then increased with pre- and post-processing times to account for cleaning, repositioning, setting up, and taking down. The total 3D print time is estimated to be 34 minutes per half blade tip, and labor costs sum up to \$40 per blade tip. Next, the model estimates material costs assuming pellet costs of \$7 kg^{-1} and a waste factor of 10%. For the 15-m blade tip, material costs sum up to \$346. Finally, the model estimates capital costs by assuming a cost per material extruded of \$150,000, a life of 10 years, and a total number of blade tips of 1,000 per year, resulting in capital costs of \$271 per blade tip. The total cost of the additive manufacturing of the outer shell reinforcement of the 15-m blade tip is expected to be \$657 with labor and cycle time of 0.6 h and 1.1 h, respectively.

D. Prefabricated Leading Edge

Leading edge erosion is a major concern for wind turbine manufacturers, owners, and operators. In addition, the leading edge is subjected to tight manufacturing tolerances that are hard to achieve during the conventional assembly

process. To alleviate both aspects, one solution consists of mounting a prefabricated leading edge at the nose of the blade tip. This solution, somewhat inspired by the automotive industry, is assumed to be part of the advanced manufacturing process, although could also be applied to standard manufacturing. Prefabricated leading edges add 28 kg of material mass, $118 of material costs, and 11 h of labor per tip. The advantages in power production and operation and maintenance costs of the prefabricated leading edge would only be quantifiable in the field and, although foreseen to be significant, a conservative approach is adopted and neglects those advantages.

IV. Comparison

The detailed comparison of bill of materials, labor, cycle time, variable costs, and fixed costs between conventional and advanced manufacturing processes for the 15-m blade tip is presented in Fig. 3 and discussed in the next sections. Please note that all the numbers are estimated as accurately as possible. Still, the advanced manufacturing process is at a much earlier stage of development than conventional manufacturing of blade tips. Therefore, several uncertainties affect the results.

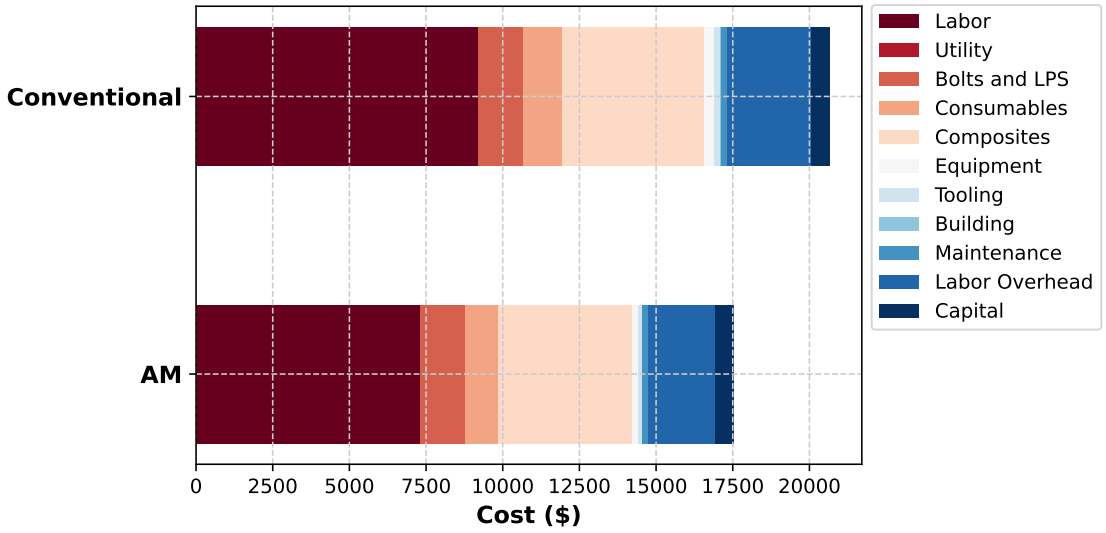

Fig. 3 Cost comparison between conventional tip and tip adopting advanced manufacturing. Variable costs include labor, utility, and materials costs, whereas fixed costs include equipment, tooling, building, maintenance, labor overhead, and capital costs.

A. Bill of Materials

The conventional and AM tip have similar masses of 580 kg and similar bills of materials. The only notable difference in mass is seen in the use of the prefabricated leading edge, which adds 28 kg in the advanced tip. The change in resin and the 3D printing of the reinforcement grid are not expected to notably impact tip mass. The impact of AM on costs is harder to estimate, and a few differences in the individual material contributions are expected. Sandwich core material accounts for $618 of cost. This number can be reduced by 40% when 3D printing the thermoplastic grid thanks to the lower unit cost of thermoplastic resin and chopped glass fibers. The accurate estimate of adhesive cost is hard to achieve, as thermoplastics require adhesives that are twice the cost, $15 kg^{-1} versus $7 kg^{-1}, and the prefabricated leading edge adds a bond line. Nonetheless, AM offers the opportunity to reduce the thickness and width of bond lines thanks to the tighter tolerances. Overall, we estimate a potential saving in adhesive cost up to 50%. Next to these reductions in costs, thermoplastic resin is expected to cost significantly more than thermoset epoxy, $6.8 kg^{-1} versus $3.6 kg^{-1}. All in all, the total bills of materials between conventional and AM blade tips are estimated to be similar—$4,600 per tip.

B. Labor and Cycle Time

Advantages for the AM tip are observed in the labor and cycle time. The conventional blade tip requires 156 h and 61 h, respectively, whereas the AM tips are manufactured in 124 h and 37 h, respectively. The faster manufacturing processes are attributed to the simpler infusion process on a flat table, as well as switching from the manual placement of the sandwich core to the 3D printing of the reinforcement grid. The infusion of the flat tip blanks is estimated to require 32 h of labor and 8 h of cycle time. The thermoforming of the skins is estimated to require 17 h of labor and 3 h of cycle time. In contrast, the conventional infusion of each shell in the mold is estimated to require 36 h of labor and 18 h of cycle time. The 3D printing of panel reinforcement is highly automated and requires only 0.6 h of labor and 1.1 h of cycle time.

C. Variable and Fixed Costs

The comparison of the variable costs reflects the 20% reduction in labor costs. Also, consumables can be reduced by 15% by infusing on a flat table and not in a curved mold. With the other contributions—namely utility costs, composite material costs, joint bolts, and lightning protection system—staying similar, baseline variable costs are estimated to be $16,600, whereas AM variable costs are estimated to be $14,200, or a 14% reduction.

Despite several uncertainties affecting the analysis, we estimate that fixed costs can also be slightly reduced thanks to AM. Equipment and tooling costs can be reduced by 30% and 50%, respectively, by infusing on flat tables, replacing the sandwich core by 3D printing the reinforcement grid, and using cheaper molds with less stringent tolerances on temperature control. Labor overhead can also be proportionally reduced by the same amount of labor hours. The capital and operation and maintenance costs of 3D printers are estimated to be limited to $136 per blade tip, and total fixed costs are estimated to decrease from $4,100 to $3,300. Overall, total cost per blade tip is estimated to drop by 15% from $20,700 to $17,500.

V. Life Cycle Environmental Impact

The functional unit used for the life cycle analysis is the finished 15-m blade tip ready for shipment to a deployment site. We selected two impact metrics in this study—climate change and cumulative energy demand (CED)—calculated by ReCiPe v1.13. and CED v1.09 impact assessment protocols, respectively [37, 38]. Climate change impact category quantifies the 100-year global warming potential (GWP) arising from greenhouse gas emissions in all examined processes, expressed in kilograms of carbon dioxide equivalent ($CO_{2\,eq}$). Cumulative energy demand quantifies embodied energy in all examined life cycle stages from fossil and renewable sources, reported in megajoules.

We quantified material, energy, and emissions input and output flows for each life cycle stage examined. For the foreground data, representing direct flows of blade tip manufacturing, we used the bill of materials reported herein to compare different material selections and quantities for both designs. We used well-known life cycle inventory (LCI) database libraries to model the life cycle flows of those materials including ecoinvent version 3.9, USLCI, and European Life Cycle Data Network [39, 40]. Some materials, such as pultruded carbon fiber and in-situ polymerizing thermoplastic resin, were not available in these LCI databases. We modeled LCI entries for missing materials by building upscaled process models leveraging available literature and industry stakeholders. Pultruded carbon fibers were modeled after the carbonization of polyacrylonitrile fibers and subsequent surface treatment and sizing. We used the European Composite Industry Association (EuCIA) Eco Impact Calculator to model pultrusion processing input and output flows [41]. Whenever possible, we substituted European inputs (i.e., electricity grid mix, transportation) with U.S.-based inputs such as Western Electricity Coordinating Council (WECC) interconnection electricity mix to model a material manufacturer and a blade manufacturer located in the United States.

Direct energy consumption of unit processes for the baseline tip design was estimated using the blade cost model in WISDEM. For the AM tip design, most processes had similar energy consumption to those in the baseline, except in three main processes: post-curing of the flat tip blanks, vacuum thermoforming of the skin panels, and 3D printing of the grid reinforcement. Estimates for the energy consumption of these steps were calculated by multiplying average process step time by the wattage of the equipment, corrected by utilization factors of relevant unit processes. The next two sections discuss the results of the life cycle impact assessment, which are summarized in Table 5.

A. Climate Change

The climate change impact of producing 15-m baseline and AM tips is 3,160 and 3,360 kg $CO_{2\,eq}$, respectively; thus, AM tip carries 6.3% higher greenhouse gas emissions along its supply chain. The bill of materials is the largest

Table 5 Environmental impact in terms of climate change and cumulative energy demand between baseline and advanced tip

Environmental Impact Category	Baseline	AM	Difference
Climate change (kg $CO_{2\,eq}$)	3,160	3,360	+6.3%
Cumulative energy demand (MJ)	49,800	51,300	+3.0%

contributor to supply chain equivalent carbon emissions. The top contributing materials to climate change are pultruded carbon fiber, dry glass fiber fabrics, and resin. Nearly one-third of the impacts is ascribed to the production of pultruded carbon fiber for the spar caps. This alone carries 12.0 kg $CO_{2\,eq}$ per kilogram of material compared to 3.2 kg $CO_{2\,eq}$ per kilogram of dry glass fiber. Since the two tips have similar bills of materials, the climate change impact is similar between the two designs. Also, since this life cycle analysis currently neglects the impact of recyclability, thermoset and thermoplastic resins have similar climate change impacts because both have similar upstream supply chain profiles stemming from crude oil extraction. Thermoset and thermoplastic resins carry 7.02 kg $CO_{2\,eq}$ and 7.04 kg $CO_{2\,eq}$ per kilogram of resin, respectively.

The marginally higher impact of AM tip can be mostly ascribed to a higher direct process energy consumption. The AM process has 30% higher direct electricity usage than its baseline counterpart; this higher energy consumption is needed to keep the mold heated during both the vacuum thermoforming of the skin panels and the 3D printing of the reinforcement grids. In addition, the 3D printers require energy to run. The process is the second highest contributor to direct energy consumption, representing 23% of total direct energy usage. The two increases in energy usage outweigh the more efficient post-curing step that AM unlocks. The post-curing is performed after the tip blanks are infused on the flat table, and the full blade tip no longer needs to go through a post-curing step as a whole component. In this project, we assumed an energy savings of 50% for post-curing. Note however that the direct energy consumption for baseline and AM tips contributes only 5% and 3.5% to the climate change impact, respectively.

B. Embodied Energy

Embodied energy, calculated by cumulative energy demand of producing the baseline and AM tip, is estimated to be 49,800 MJ and 51,300 MJ, respectively. The AM tip carries a 3.0% higher embodied energy than the baseline tip. Non-renewable fossil energy is the main form of embodied energy; this is ascribed to reliance on upstream oil and gas operations for supply of petrochemical precursors to resin and fiber production and, to a lesser extent, electricity and heat production. The thermoset resin has embodied energy of 135 MJ kg^{-1}, whereas the thermoplastic resin has 120 MJ kg^{-1}. Similar contributing factors for higher climate change potential for the AM tip also hold for the embodied energy category.

VI. Conclusions

This paper presents a techno-economic analysis and life cycle analysis comparing a standard process and an advanced process for the design and manufacturing of a 15-m tip of an 80-m-long wind turbine blade representative of modern land-based configurations. The advanced manufacturing process is motivated by the need to limit costs, labor hours, and cycle times and increase factory throughput, production quality, and consistency. The process is based on the thermoforming of flat tip blanks made of thermoplastic material, the 3D printing of a reinforcement grid replacing conventional sandwich foam, and the installation of a prefabricated leading edge. The comparison between the two processes shows that the tip adopting advanced manufacturing has a lower labor by 21%, lower cycle time by 39%, and lower total blade tip costs by 15% while simultaneously increasing production quality and adopting recyclable in-situ polymerizing thermoplastic resin. The life cycle analysis shows mild increases of 6.3% kg $CO_{2\,eq}$ and 3.0% cumulative energy demand for the AM tip, caused by the higher energy usage needed to manufacture the AM tip.

Work is currently ongoing to include recyclability into the life cycle analysis of standard and advanced blade tips. In the meantime, advanced blade tips are being tested in the laboratory to validate and certify compliance with their structural requirements. Field testing of a wind turbine mounting advanced blade tips is also planned.

Acknowledgments

The guidance of multiple experts at GE Global Research, GE Renewable Energy, LM Wind Power, and Sandia National Laboratories has been extremely valuable. A portion of the research was performed using computational resources sponsored by the U.S. Department of Energy's Office of Energy Efficiency and Renewable Energy and located at the National Renewable Energy Laboratory. This work was authored in part by the National Renewable Energy Laboratory, operated by Alliance for Sustainable Energy, LLC, for the U.S. Department of Energy (DOE) under Contract No. DE-AC36-08GO28308. Funding provided by the U.S. Department of Energy Office of Energy Efficiency and Renewable Energy Advanced Materials and Manufacturing Technologies Office, Award Number DE-EE0009403. The views expressed in the article do not necessarily represent the views of the DOE or the U.S. Government. The U.S. Government retains and the publisher, by accepting the article for publication, acknowledges that the U.S. Government retains a nonexclusive, paid-up, irrevocable, worldwide license to publish or reproduce the published form of this work, or allow others to do so, for U.S. Government purposes.

References

[1] Bolinger, M., Lantz, E., Wiser, R., Hoen, B., Rand, J., and Hammond, R., "Opportunities for and challenges to further reductions in the "specific power" rating of wind turbines installed in the United States," *Wind Engineering*, 2020, p. 0309524X19901012. https://doi.org/10.1177/0309524X19901012.

[2] Wiser, R., Bolinger, M., Hoen, B., Millstein, D., Rand, J., Barbose, G., Darghouth, N., Gorman, W., Jeong, S., and Paulos, B., "Land-Based Wind Market Report: 2022 Edition," 2022. https://doi.org/10.2172/1882594.

[3] Cousins, D. S., Suzuki, Y., Murray, R. E., Samaniuk, J. R., and Stebner, A. P., "Recycling glass fiber thermoplastic composites from wind turbine blades," *Journal of Cleaner Production*, Vol. 209, 2019, pp. 1252–1263. https://doi.org/https://doi.org/10.1016/j.jclepro.2018.10.286.

[4] Veers, P., Bottasso, C., Manuel, L., Naughton, J., Pao, L., Paquette, J., Robertson, A., Robinson, M., Ananthan, S., Barlas, A., Bianchini, A., Bredmose, H., Horcas, S. G., Keller, J., Madsen, H. A., Manwell, J., Moriarty, P., Nolet, S., and Rinker, J., "Grand Challenges in the Design, Manufacture, and Operation of Future Wind Turbine Systems," *Wind Energy Science Discussions*, Vol. 2022, 2022, pp. 1–102. https://doi.org/10.5194/wes-2022-32.

[5] Bortolotti, P., Berry, D. S., Murray, R., Gaertner, E., Jenne, D. S., Damiani, R. R., Barter, G. E., and Dykes, K. L., "A Detailed Wind Turbine Blade Cost Model," 2019. https://doi.org/https://dx.doi.org/10.2172/1529217.

[6] Johnson, S. B., Chetan, M., Griffith, D. T., and Sherwood, J. A., "Development of high-fidelity design-driven wind blade manufacturing process models to investigate labor predictions in wind blade manufacture," *Wind Energy*, Vol. 25, No. 8, 2022, pp. 1313–1331. https://doi.org/https://doi.org/10.1002/we.2731.

[7] Galos, J., Das, R., Sutcliffe, M. P., and Mouritz, A. P., "Review of balsa core sandwich composite structures," *Materials Design*, Vol. 221, 2022, p. 111013. https://doi.org/https://doi.org/10.1016/j.matdes.2022.111013.

[8] Compton, B. G., and Lewis, J. A., "3D-Printing of Lightweight Cellular Composites," *Advanced Materials*, Vol. 26, No. 34, 2014, pp. 5930–5935. https://doi.org/https://doi.org/10.1002/adma.201401804.

[9] Zaharia, S. M., Enescu, L. A., and Pop, M. A., "Mechanical Performances of Lightweight Sandwich Structures Produced by Material Extrusion-Based Additive Manufacturing," *Polymers*, Vol. 12, No. 8, 2020. https://doi.org/10.3390/polym12081740.

[10] Hu, C., and Qin, Q.-H., "Advances in fused deposition modeling of discontinuous fiber/polymer composites," *Current Opinion in Solid State and Materials Science*, Vol. 24, No. 5, 2020, p. 100867. https://doi.org/https://doi.org/10.1016/j.cossms.2020.100867.

[11] Fink, J., *Methods of 3D Printing*, John Wiley Sons, Ltd, 2018, Chap. 1, pp. 1–60. https://doi.org/https://doi.org/10.1002/9781119555308.ch1.

[12] Kunc, V., Lindahl, J., Hershey, C., Kastura, M., Walch, M., and De luca, T., "Additive Manufacturing of Thermoset Cellular Structures," 2019. https://doi.org/10.2172/1530085.

[13] Bandyopadhyay, . B. S., A., *Additive Manufacturing, Second Edition*, CRC Press, https://doi.org/10.1201/9780429466236. https://doi.org/2019.

[14] Nguyen, N. A., Barnes, S. H., Bowland, C. C., Meek, K. M., Littrell, K. C., Keum, J. K., and Naskar, A. K., "A path for lignin valorization via additive manufacturing of high-performance sustainable composites with enhanced 3D printability," *Science Advances*, Vol. 4, No. 12, 2018, p. eaat4967. https://doi.org/10.1126/sciadv.aat4967.

[15] Duty, C. E., Drye, T., and Franc, A., "Material Development for Tooling Applications Using Big Area Additive Manufacturing (BAAM)," 2015. https://doi.org/10.2172/1209207.

[16] Ngo, T. D., Kashani, A., Imbalzano, G., Nguyen, K. T., and Hui, D., "Additive manufacturing (3D printing): A review of materials, methods, applications and challenges," *Composites Part B: Engineering*, Vol. 143, 2018, pp. 172–196. https://doi.org/https://doi.org/10.1016/j.compositesb.2018.02.012.

[17] Ligon, S. C., Liska, R., Stampfl, J., Gurr, M., and Mülhaupt, R., "Polymers for 3D Printing and Customized Additive Manufacturing," *Chemical Reviews*, Vol. 117, No. 15, 2017, pp. 10212–10290. https://doi.org/10.1021/acs.chemrev.7b00074.

[18] Forster, A., "Materials Testing Standards for Additive Manufacturing of Polymer Materials: State of the Art and Standards Applicability," , 2015-05-15 2015. https://doi.org/https://doi.org/10.6028/NIST.IR.8059.

[19] Caminero, M., Chacón, J., García-Moreno, I., and Reverte, J., "Interlaminar bonding performance of 3D printed continuous fibre reinforced thermoplastic composites using fused deposition modelling," *Polymer Testing*, Vol. 68, 2018, pp. 415–423. https://doi.org/https://doi.org/10.1016/j.polymertesting.2018.04.038.

[20] Blok, L., Longana, M., Yu, H., and Woods, B., "An investigation into 3D printing of fibre reinforced thermoplastic composites," *Additive Manufacturing*, Vol. 22, 2018, pp. 176–186. https://doi.org/https://doi.org/10.1016/j.addma.2018.04.039.

[21] Li, J., Durandet, Y., Huang, X., Sun, G., and Ruan, D., "Additively manufactured fiber-reinforced composites: A review of mechanical behavior and opportunities," *Journal of Materials Science Technology*, Vol. 119, 2022, pp. 219–244. https://doi.org/https://doi.org/10.1016/j.jmst.2021.11.063.

[22] Nissen, P. J., J., and Chiang, T., "Methods of customizing, manufacturing, and repairing a rotor blade using additive manufacturing processes - US Patent No. 10,633,976," , 2020.

[23] Tobin, M. T., J., and Anderson, T., "Methods for manufacturing wind turbine rotor blade panels having printed grid structures - US Patent No. 10,913,216," , 2021.

[24] Beyerle, J. K. P. B., P., and Thrasher, T., "Assemblies formed by additive manufacturing, radar absorbing structures, and related methods - US Patent No. 11,135,763," , 2021.

[25] Rivera, J., "Methods of forming and assembling a rotor blade using additive manufacturing processes - US Patent No. 11,427,350," , 2022.

[26] Griffin, D., "Creating Pathways to Success for Supersized Wind Turbine Blades: 2018 Workshop Summary Report," 2018. https://doi.org/10.2172/1439243.

[27] Post, B., Atkins, C., Jackson, A., Chesser, P., Roschli, A., Barnes, A., Nycz, A., Meyer, L., Jensen, P., Vcelka, M., and Carron, S., "A Comparative Study of Direct and Indirect Additive Manufacturing Approaches for the Production of a Wind Energy Component," 2021. https://doi.org/10.2172/1809969.

[28] ISO, "ISO 14040:2006 - Environmental management - Life cycle assessment - Principles and framework," , 2022. URL https://www.iso.org/standard/37456.html.

[29] Bortolotti, P., Tarres, H. C., Dykes, K. L., Merz, K., Sethuraman, L., Verelst, D., and Zahle, F., "IEA Wind TCP Task 37: Systems Engineering in Wind Energy - WP2.1 Reference Wind Turbines," 2019. https://doi.org/10.2172/1529216.

[30] Smith, K. J., and Griffin, D. A., "Supersized Wind Turbine Blade Study: RD Pathways for Supersized Wind Turbine Blades," 2019. https://doi.org/10.2172/1498695.

[31] Carron, W. S., and Bortolotti, P., "Innovative rail transport of a supersized land-based wind turbine blade," *Journal of Physics: Conference Series*, Vol. 1618, No. 4, 2020, p. 042041. https://doi.org/10.1088/1742-6596/1618/4/042041.

[32] Bortolotti, P., Johnson, N., Abbas, N. J., Anderson, E., Camarena, E., and Paquette, J., "Land-based wind turbines with flexible rail-transportable blades – Part 1: Conceptual design and aeroservoelastic performance," *Wind Energy Science*, Vol. 6, No. 5, 2021, pp. 1277–1290. https://doi.org/10.5194/wes-6-1277-2021.

[33] Peeters, M., Santo, G., Degroote, J., and Paepegem, W. V., "The Concept of Segmented Wind Turbine Blades: A Review," *Energies*, Vol. 10, No. 8, 2017. https://doi.org/10.3390/en10081112.

[34] Anderson, B., Bortolotti, P., and Johnson, N., "Development of an open-source segmented blade design tool," *Journal of Physics. Conference Series*, Vol. 2265, No. 3, 2022. https://doi.org/10.1088/1742-6596/2265/3/032023.

[35] Bortolotti, P., Dixon, K., Gaertner, E., Rotondo, M., and Barter, G., "An efficient approach to explore the solution space of a wind turbine rotor design process," *Journal of Physics. Conference Series*, Vol. 1618, 2020. https://doi.org/10.1088/1742-6596/1618/4/042016.

[36] Stehly, T., and Duffy, P., "2020 Cost of Wind Energy Review," 2021. https://doi.org/10.2172/1838135, URL https://www.osti.gov/biblio/1838135.

[37] Huijbregts, M., Steinmann, Z., Elshout, P., Stam, G., Verones, F., Vieira, M., Zijp, M., Hollander, A., and Zelm, R., "ReCiPe2016: a harmonised life cycle impact assessment method at midpoint and endpoint level," *The International Journal of Life Cycle Assessment*, Vol. 22, 2016. https://doi.org/10.1007/s11367-016-1246-y.

[38] Frischknecht, R., Wyss, F., Knöpfel, S., Lützkendorf, T., and Balouktsi, M., "Cumulative energy demand in LCA: the energy harvested approach," *The International Journal of Life Cycle Assessment*, Vol. 20, 2015. https://doi.org/10.1007/s11367-015-0897-4.

[39] "ecoinvent 3.5; Swiss Center for Life Cycle Inventories," , 2019. URL https://ecoinvent.org/the-ecoinvent-database/data-releases/ecoinvent-3-5/.

[40] NREL, "U.S. Life Cycle Inventory Database," , 2022. URL https://www.nrel.gov/lci/.

[41] "EuCIA Eco Impact Calculator," , 2022. URL https://ecocalculator.eucia.eu/Account/Login?ReturnUrl=%2F.